



ELSEVIER

Available online at www.sciencedirect.com

SCIENCE @ DIRECT®

Palaeogeography, Palaeoclimatology, Palaeoecology 216 (2005) 267–277

PALAEO

www.elsevier.com/locate/palaeo

Terminations and their correlation with solar insolation in the Northern Hemisphere: a record from a loess section in Northwest China

Guangjian Wu^{a,b,*}, Baotian Pan^c, Qingyu Guan^c, Dunsheng Xia^d

^a*Institute of Tibetan Plateau Research, Chinese Academy of Sciences, Beijing 100085, China*

^b*Key Laboratory of Ice Core and Cold Regions Environment, Cold and Arid Regions Environmental and Engineering Research Institute, CAS, Lanzhou, Gansu 730000, China*

^c*School of Resource and Environment, National Laboratory of Western China's Environmental Systems, Lanzhou University, Lanzhou, Gansu 730000, China*

^d*Key Laboratory of Desert and Desertification, Cold and Arid Regions Environmental and Engineering Research Institute, CAS, Lanzhou, Gansu 730000, China*

Received 26 March 2003; received in revised form 2 September 2004; accepted 5 November 2004

Abstract

A high-resolution loess section in Northwest China is analyzed for the major climate terminations and their correlation with solar insolation over the past 0.8 Ma. Based on age controls and a grain size age model proposed by Porter and An (Porter, S.C., An, Z.S., 1995. Correlation between climate events in the North Atlantic and China during the last glaciation. *Nature* 375, 305–308.), a timescale for the Shagou loess section is constructed, which is independent of orbital tuned results. The timescale is similar to other loess sections, and the mid-point ages of the boundary between a paleosol and its underlying loess layer are very close to that of terminations recorded in the marine record. Shagou section records indicate that grain size changed sharply during the termination process. Terminations occurred at the time of the maximum or increase of July radiation in the Northern Hemisphere at high latitudes, suggesting that insolation might be a factor affecting terminations in the Chinese loess. This result supports the Milankovitch hypothesis. However, variations in the amplitude of the insolation and grain size records are not proportionally matched, so that the mechanism remains unsolved.

© 2004 Elsevier B.V. All rights reserved.

Keywords: Loess; Grain size; Termination; Insolation

1. Introduction

The Milankovitch hypothesis holds that global climate is forced by solar radiation received by the earth. Marine oxygen isotope records display the

* Corresponding author. Institute of Tibetan Plateau Research, Chinese Academy of Sciences, No. 18 Shuangqing Road, Beijing 100085, China.

E-mail address: wugj@itpcas.ac.cn (G. Wu).

correlation between global ice volume and earth orbit, the latter directly regulating the solar insolation received by the earth's surface (Hays et al., 1976). Though there are problems with the Milankovitch hypothesis, such as the mechanism by which and the degree to which insolation plays a role in global and regional climate, it is widely accepted. Abundant evidence has also been provided in support of this hypothesis by Chinese loess records (Liu et al., 1999). For example, solar insolation might be a forcing factor on the East Asian winter monsoon variations by way of ice volume changes (Ding et al., 1995). Over the last 150 ka, precipitation in July on the Loess Plateau has shown close correlation with radiation in lower latitudes (Lu et al., 1996). The response of mollusk assemblages to orbital forcing in the last 250 ka has been reported from Luochuan loess section (Wu et al., 2000). However, arguments also exist that question the validity of this hypothesis (Winograd et al., 1992, 1997; Muller and MacDonald, 1997).

In China, loess layers were deposited during cold and arid glacial periods (during even-numbered marine isotope stages, MIS), and paleosols developed during warm-moist interglacials (during odd-numbered MIS; Liu et al., 1985), the loess–paleosol sequences thus recording the glacial–interglacial cycles. The boundary between a paleosol and its underlying loess layer reflects the transition from glacial to interglacial, although eolian sediment may be subjected to alteration by post-depositional leaching and pedogenic process to some degree, especially with a climatic shift from glacial to interglacial. This may cause some uncertainties at the paleosol–loess boundaries, since loess deposition is continuous between glacial and interglacial periods. In the western part of the Chinese Loess Plateau, the loess accumulation rate was high and the record provides a stratigraphy containing few disruptions. Therefore, loess records from this area are useful in discussing the transitions from glacial to interglacial periods, i.e., the terminations, including their amplitudes and phases. In this paper, information on terminations over the past 800 ka from a loess section in northwest China and their main characteristics are discussed. If the timing of terminations in loess deposit is correlated with solar insolation, then it can provide support to the Milankovitch hypothesis.

2. Stratigraphy and age dating

The Shagou loess section (37°33' N, 102°49' E) is situated on the northern flank of Qilian Mountains, Hexi (Gansu) Corridor, close to the Tengger Desert (Fig. 1). The total thickness of the Quaternary section of Shagou is about 230 m. The loess–paleosol sequences in the section compare well with those in the central Chinese Loess Plateau from L9 at the bottom to L1 at the top. The Holocene deposit is largely absent because of post-depositional denudation. Paleosols are less well developed compared to those in the central Loess Plateau with weak carbonate leaching and less clay material. Mean annual temperature and precipitation are about 5 °C and 300 mm, respectively. Disruption at contacts between paleosols and the underlying loess layers is quite rare because of minimal bioturbation, weak post-depositional pedogenesis, and weak runoff. The unusually high accumulation rate (about 230 m/820 ka) would have also served to minimize the extent and degree of post-depositional alteration. Thus, records of terminations (deglaciations) are well preserved.

Samples were taken at 10-cm intervals from L2 to the bottom of the Shagou section, at 5-cm intervals for the S2 paleosol and the L2 and L1 loess layers, and at 2.5-cm intervals for the S1 paleosol. Theoretically, the resolution is within ~1 ka below S1, and 0.1–0.2 ka for S1 and L1. Grain size is a sensitive proxy index of the winter monsoon and its response time to climatic changes in the Chinese loess deposit is very short (Derbyshire et al., 1997); here, it is the chosen climate proxy when discuss the terminations. Grain size measurements ranging from 0.02–2000 µm were completed using a Malvern Mastersizer 2000. Organic matter and carbonates were removed before grain measuring. The measurement precision ($n=15$) of the median grain size and the sand content for a sample from the lower part of the S1 paleosol is 1.115% and 2.727%, respectively.

A chronology for the Shagou section was established using paleogeomagnetic, radiocarbon dating, and TL dating. Previous work suggested that the age of the base of the Shagou section is about 0.83 Ma, i.e., older than the Brunhes/Matuyama boundary (Pan et al., 2001). All the TL dating results were completed at the State Key Laboratory of Loess and Quaternary Geology, Xi'an, while all the ^{14}C dating results were

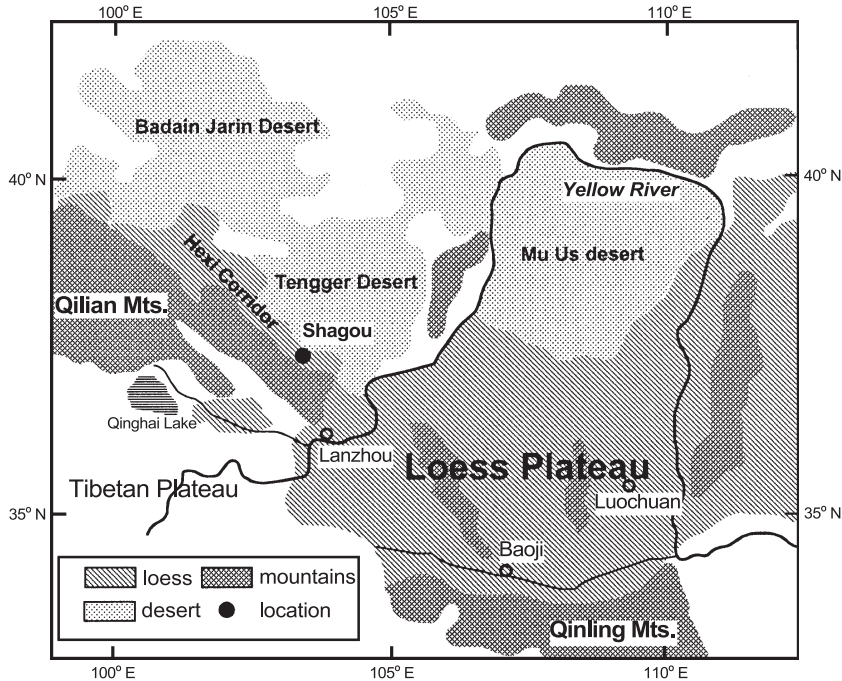


Fig. 1. Location of the Shagou, Baoji, and Louchuan loess sections.

completed at Lanzhou University. The TL dating ages for the bottom and top of S2 are 248 ± 19 ka and 197 ± 19 ka, respectively, those for S1 are 131 ± 10 ka and 61 ± 5 ka, respectively (Wu et al., 2002). In addition, the ^{14}C age for the top of L1 is 13 ± 0.28 ka. These dating results confirm with those from the lithostratigraphy (Fig. 2).

3. Setting up the timescale

Timescales for loess–paleosol sequences are mainly obtained using models with some “standard” age controls or a target curve that was generally developed by orbital tuning or absolute dating. Because the measurements are imprecise, the above TL and radiocarbon dating results cannot be used as age controls to set up a timescale for Shagou section. The Brunhes/Matuyama boundary is taken as a non-tuned age control, set at 780 ka (Cande and Kent, 1995). No other paleogeomagnetic reversals have been found between the Brunhes/Matuyama boundary and the top of the Shagou section, so other age controls must be sought. The SPECMAP timescale

has been a benchmark for paleoclimate studies. Based on the concentration of radiocarbon in the atmosphere, a new dating result for the Younger Dryas events has been obtained (12,700–11,500 aBP, Golsar et al., 2000). We take the end of the Younger Dryas event as the MIS 2/1 boundary, but we retain the use of the SPECMAP (Martinson et al., 1987) and the MD900963+ODP677 timescale (Bassinot et al., 1994) for the older boundaries. In order to set up a timescale that is as independent as possible of the tuned records, the tuned age controls must be minimized. Age controls adopted in this paper, and comparisons with the dating results, are shown in Table 1 and Fig. 2.

The age of a given level in the Shagou loess section between the neighboring two age controls is calculated using the grain size age model of Porter and An (1995), which assumes that the dust flux is proportional to grain size. For those strata below the Brunhes/Matuyama boundary, ages are calculated by extrapolation, using the 242 ka and 780 ka age controls. Different grain size parameters can be used in this model (Vandenberghe et al., 1997; Lu et al., 1997). In this paper, the $>40 \mu\text{m}$ fraction and median particle size (Md), as suggested by Porter and An

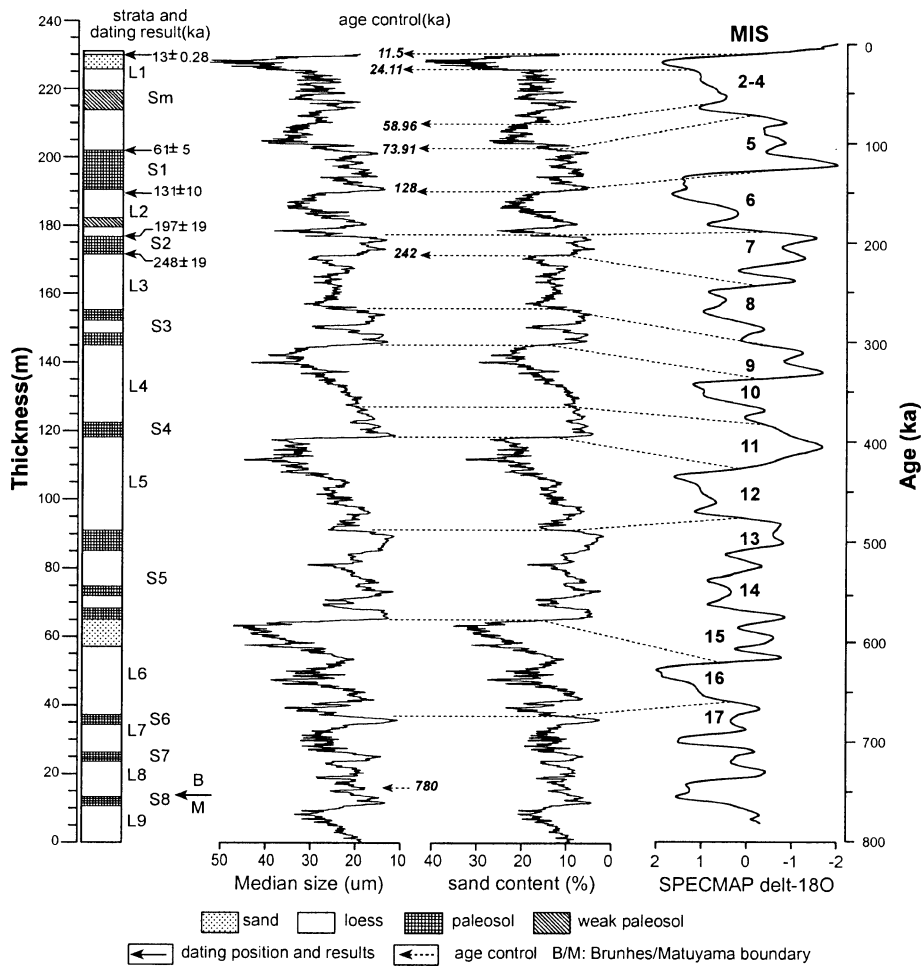


Fig. 2. Stratigraphy, grain size records (3-point smoothing), dating results and age controls for the Shagou loess section, compared with the SPECMAP record.

(1995), are used in the model. The difference between the two results is very small. In the S1 paleosol and the L1 loess layer, the maximal age difference for the same sample is less than 0.2 kyr, the difference for the remaining period being less than 3.5 kyr. The $>40 \mu\text{m}$ fraction timescale is finally used for Shagou section.

Paleogeomagnetic samples were taken at 1-m intervals, so that the location of the Brunhes/Matuyama boundary has a maximal error of ± 1 m. The age uncertainty caused by the paleogeomagnetic sampling interval decreases closer to the top of the section. Using the timescale based on the $>40 \mu\text{m}$ fraction, the maximal age uncertainty arising from this

is less than 3.4 ka at the MIS 16/15 boundary, corresponding to Termination VII.

Table 2 shows the timescale of the Shagou section and is compared to three selected loess sections in the Loess Plateau and the marine record. Orbital results are from Ding et al. (1994) and Lu et al. (1999). The former used a grain size record as the target curve, while the latter used a magnetic susceptibility record. The results of the grain size age model are from Lu et al. (1997) and this work.

It can be seen from Table 2 that the boundary ages of loess and paleosols sequences at Shagou, calculated using the grain size age model, are generally similar to the other selected loess sections and the marine

Table 1
Age controls and their positions in the Shagou loess section

Boundaries	Position (m)	Dating result (ka)	Age control (ka)	Reference
MIS 2/1 (L1/So)	229.975	13±0.28(¹⁴ C)	11.5	Golsar et al., 2000
MIS 3/2	225.925		24.11	Martinson et al., 1987
MIS 4/3	210.525		58.96	Martinson et al., 1987
MIS 5/4 (S1/L1)	202.125	61±5(TL)	73.91	Martinson et al., 1987
MIS 6/5 (L2/S1)	190.525	131±10(TL)	128	Martinson et al., 1987
MIS 8/7 (L2/S2)	171.65	248±19(TL)	242	Bassinot et al., 1994
B/M	13	B/M (Paleogeomag.)	780	Cande and Kent, 1995

record. It should be pointed out that the Brunhes/Matuyama boundary is set at 730 ka by Ding et al. (1994) and Lu et al. (1997), while Bassinot et al. (1994), Lu et al. (1999) and the authors of this paper set it at 780 ka. In records older than the MIS 16, this may be the main cause for age difference. The timescales of the tuned MD900963+ODP677 stacked record and the Shagou section are very similar. Obvious differences occur at the top of the S4

paleosol (MIS 11/10), top of the S5 (MIS 13/12) and the S6 paleosols (MIS 17/16), respectively, with discrepancies of 26 ka, 27 ka and 35 ka. However, for each termination (corresponding to the base of the paleosols), the age differences are very minor. Both in the SPECMAP and MD900963+ODP677 timescales, the mid-point age of Termination VI is set at ~620 ka. This agrees with the result from the Shagou section but differs from all three selected loess sections in the Loess Plateau. The grain size age model provides a reliable timescale for the Shagou loess section, although use of this model is generally confined to the last glacial–interglacial cycle.

Fig. 3 shows the solar insolation curve at 65°N (Berger and Loutre, 1991) compared to the median grain size for the Shagou section with independent timescale. It is interesting that the grain size record fits insolation closely in the eccentricity cycle, while not perfectly in the precession cycle, especially during the period between MIS 6 and MIS 16. We suspect that precession plays only a minor role in the climate record at Shagou, as it is situated in the mid-latitudes. However, the terminations are tightly associated with increases or peaks of insolation in the northern hemisphere high latitudes, suggesting that the 100 kyr eccentricity is the dominating cycle in the Shagou

Table 2
Paleosol ages from different studies and comparison with the marine record (unit: ka)

Strata	Baoji (Ding et al., 1994)	Luochuan (Lu et al., 1997)	Luochuan (Lu et al., 1999)	Shagou (this paper)	MD900963+ODP677 (Bassinot et al., 1994)	
S0 bottom	11			<u>11.5</u>	MIS2/1	11
S1 top	72	73	71	<u>73.91</u>	MIS5/4	71
S1 bottom	128	129	129	<u>128</u>	MIS6/5	127
S2 top	190	196	188	<u>196</u>	MIS7/6	186
S2 bottom	250	246	254	<u>242</u>	MIS8/7	242
S3 top	282	284	279	288	MIS9/8	301
S3 bottom	334	330	334	332	MIS10/9	334
S4 top	388	368	385	390	MIS11/10	364
S4 bottom	418	408	428	424	MIS12/11	427
S5 top	482	476	471	501	MIS13/12	474
S5 bottom	579	560	576	622	MIS16/15	621
S6 top	648	638	658	694	MIS17/16	659
S6 bottom	667	666	670	708	MIS18/17	712
S7 top	727	696	706	732		
S7 bottom	742	735	748	741		
S8 top	762	740	760	776		
S8 bottom	792	792	788	789		

Underlined numbers are age controls. The ages of boundaries between MIS in Bassinot et al. (1994) are equivalent to isotope events 2.0, 6.0, 8.0, 10.0, 12.0, 14.0, 16.0 and 18.0.

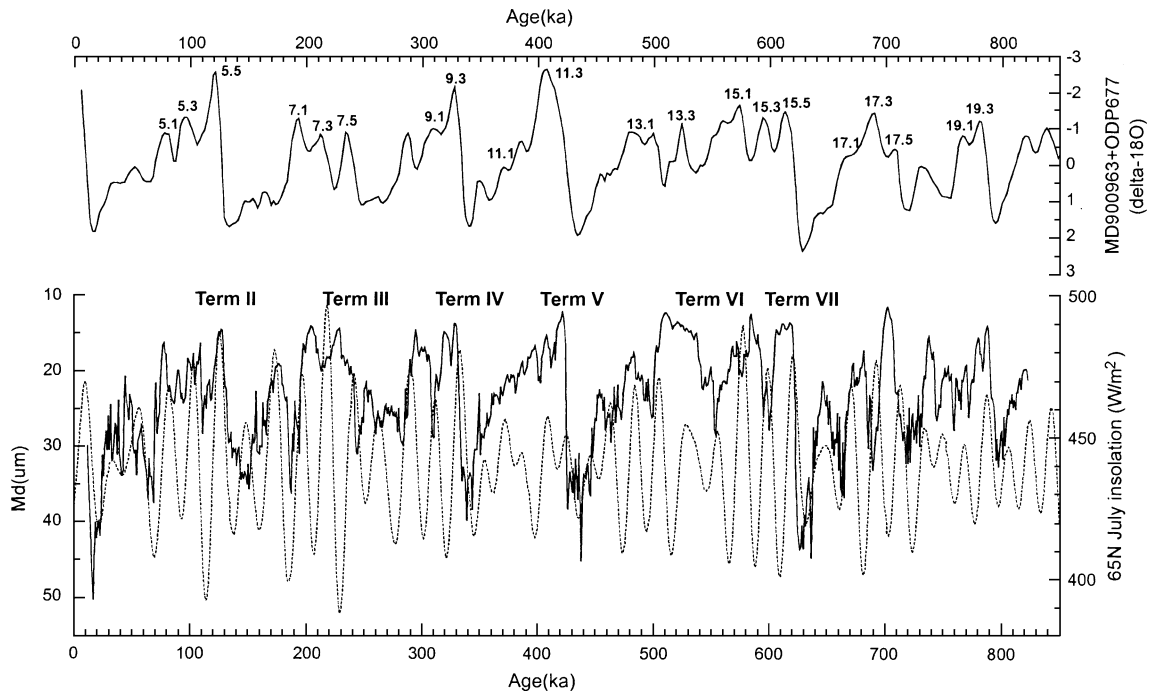


Fig. 3. Comparison of median grain size record of Shagou section (solid line, calculated using the $>40\ \mu\text{m}$ fraction), global ice volume (solid line, Bassinot et al., 1994), and solar insolation in July at 65°N (dashed line, Berger and Loutre, 1991).

record. Results of spectrum analysis for the Shagou section agree with earth orbital cycles. The main cycles are 101 kyr, 40.5 kyr and 90 kyr. The 101 kyr and 90 kyr cycles correspond to eccentricity, while the 40.5 kyr to obliquity, although the precession signal is rather weak.

4. Terminations recorded in the Shagou section and relation to solar insolation

4.1. Amplitude

From MIS 16, corresponding to L6, the grain size record indicates that the particles become coarser from the bottom upwards in every loess layer. This characteristic is similar to the marine oxygen isotope and global ice volume records. It is expected that growth of the Northern Hemisphere ice sheets would affect the Chinese loess deposition by enhancing the Siberian High (Ding et al., 1995). The winter monsoon would strengthen and desert margins would expand, keeping pace with the ice volume.

A clear characteristic of the Shagou section is a sharp transition from glacial to interglacial periods. The boundary of a paleosol and its underlying loess layer is very clear because post-depositional pedogenesis has been weak. In each termination, median size decreases very rapid, especially in Termination V and Termination VII. The last deglaciation (Termination I) was apparently more complex process and included Allerod and Bolling warm events and the Younger Dryas cold event. It has also been reported that Termination II was similarly complex (e.g., Seidenkrantz et al., 1996; Lotoskaya and Ganssen, 1999). In the Shagou section, the penultimate deglaciation (Termination II) seems to have an intermediate state between the penultimate glacial and the last interglacial. Such complexity can also be seen in Termination IV, although it is not so obvious. However, the overall trends of terminations are rapid, especially in Termination V and VII (Fig. 4).

Termination VII (MIS 16/15, L6/S5 boundary), Termination V (MIS 12/11, L5/S4 boundary) and Termination IV (MIS 10/, L4/S3 boundary) are very prominent. MIS 16 is the stage of the first and also the

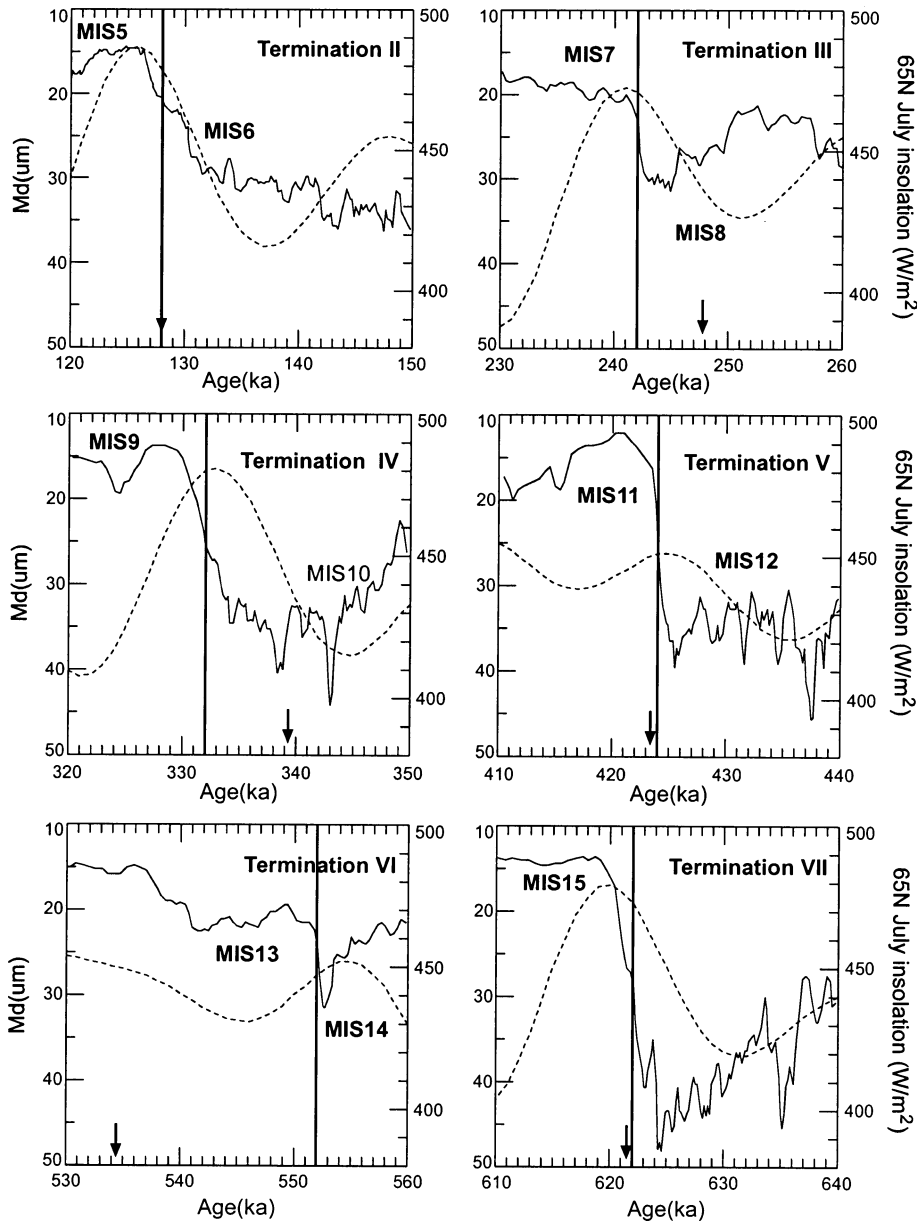


Fig. 4. Comparison of terminations recorded in the Shagou section (solid line) with solar insolation at 65°N (dashed line). Bold vertical lines and arrows indicate the mid-point age of terminations in the Shagou record and the ODP849 with GSS97 timescale (Raymo, 1997), respectively.

maximum typical glaciation after the mid-Pleistocene climate transition. Though MIS 15.5 was not as warm as MIS 11.3, MIS 9.3 and MIS 5.5, Termination VII, which is the transition between MIS 16 and MIS 15, is of maximal amplitude. In the Shagou section, L6 is the coarsest loess layer after L1, while the S5 paleosol

is the most fully developed and is the markerbed of the Chinese loess sequence (Kukla and An, 1989). Environmental contrasts between L6 and S5 increased the amplitude of Termination VII. During this termination, the median size decreased by 30 μm, and sand content dropped by 25%.

The MIS 12/11 transition has been suggested as perhaps the most severe glacial–interglacial transition over the past 0.5 Ma (Howard, 1997). MIS 12 was the coldest glacial in the past 500 ka (Raymo et al., 1990), while MIS 11 may have been the warmest interglacial in the late Pleistocene. Such a sharp contrast adds amplitude to the MIS 12/11 transition. During Termination V at Shagou, the median grain size decreased from 40 μm to 15 μm and sand content also dropped from 28% to 7%. The amplitude of Termination V was smaller than Termination VII, but greater than the other terminations.

Amplitudes of Termination III and Termination VI are small. Median grain size decreased from 30 μm at the end of MIS 8 to 20 μm in the early part of MIS 7, with amplitude of about 10 μm . The situation was similar in Termination VI. For these two terminations, the change in the marine oxygen isotope record is small. The Vostok ice core record also reveals that the amplitude of Termination III is much smaller, in both the $\delta^{18}\text{O}_{\text{sw}}$ and $\delta^{18}\text{O}_{\text{atm}}$ records (Petit et al., 1999). Indeed, Termination III and VI may not be terminations in the true sense of the word (Broecker, 1984). The characteristics of Termination VI may lie in the particularity of MIS 14, which is not a typical or extreme glaciation, with the least global ice volume after the mid-Pleistocene climate transition. In loess–paleosol sequences, Termination VI is located in the S5 paleosol. The typical S5 paleosol is a threefold polygenetic solum with two intercalated loess layers (Kukla and An, 1989). Although the S5 paleosol extends through the MIS 15, 14 and 13, and contains Termination VI, the contrast between sub-paleosols and sub-loess layers in S5 is weaker than in typical paleosol and loess layers. This may reflect the low amplitude of Termination VI in grain size records. Less glacial ice existed in MIS 8 than in MIS 16, 12, 10 and 2. This may be one of the causes of the low amplitude of Termination III.

Although the Holocene deposit is largely absent because of post-depositional denudation, the strong amplitude can be seen in the record of Termination I (the last deglaciation), reflecting the extreme environmental contrast between the last glacial maximum and the Holocene.

The relationship between of the grain size amplitude changes and insolation variations for the terminations is complex. Solar insolation changed severely

during Terminations VII, IV and II, and grain size in the Shagou section accordingly changed noticeably. For the slight variations in insolation during Termination VI and III, the grain size was of low amplitude. However some contrary indications can also be seen in the insolation record. In Termination V, solar insolation increased much less in other terminations, while the amplitude of Termination V is both stronger and larger than that of Termination III and VI. The exceptional case of MIS 12/11 transition is also found in the marine isotope records. The “MIS 11 problem,” comprising of an extraordinary warm period with low insolation during the MIS 11 stage, is still a mystery (Burckle, 1993). Termination II had an insolation variation similar to Termination VII, but its median grain size change was weaker than the latter. This indicates that insolation and global climate are not completely matched proportionally in amplitude change.

4.2. The phase

Since the tuned age controls adopted here lie at the boundaries of MIS 6/5 and MIS 8/7, Termination II and III will not be discussed in respect of their temporal correlation with solar insolation. However, the ages of Termination IV, V, VI and VII are calculated using the model and can be compared with insolation as an independent variable. It is very clear that terminations recorded in the Shagou section are closely correlated with increasing summer solar insolation in the Northern Hemisphere (Fig. 4). The mid-point ages of Termination IV, V and VI are 332 ka, 424 ka, 552 ka, respectively, exhibiting a slight lag behind the insolation maxima at 65°N in summer. The mid-point age of Termination VII is 622 ka, which slightly precedes the insolation maximum in the Northern Hemisphere. The arrows in Fig. 4 indicate the mid-point age of the ODP site 849 with the GSS97 timescale, which is also independent of orbital tuning (Raymo, 1997). Terminations both in the Shagou section and the ODP 849 have similar mid-point ages with the same insolation maxima, especially for Termination V and VII. Termination VI, however, is the only exception; its mid-point age at Shagou is a precession ahead of that in the ODP 849 timescale. This may be the result of the particularity of Termination VI and/or paleosol S5 as discussed above.

It has been pointed out that different grain size parameters may result in different timescales when using a grain size age model. Timescales calculated using median grain size and the $>40\ \mu\text{m}$ fraction are very similar. The mid-point age of terminations in the two timescales is essentially the same, because they are correlated with the same maximum of insolation. The greatest difference, which appears at Termination VII, is less than 4 kyr. In timescales calculated using median particle size, the mid-point age of Termination VII lags the insolation maximum at 65°N by about 2 kyr.

5. Discussion

It is very difficult, using the Milankovitch hypothesis, to explain why such a weak variation in solar radiation could trigger the major glacial–interglacial cycles. If solar insolation impacts global climate via the ice sheet, the ice should contain instabilities to trigger and amplify terminations (Ruddiman et al., 1989). Records from the Vostok ice core suggest two amplifiers, greenhouse gases and deglaciation enhancement by way of ice-albedo feedback, trigger terminations along with orbital forcing (Petit et al., 1999). The $\delta^{18}\text{O}$ record of groundwater at Devils Hole (DH-11) indicates that terminations do not always correlate with the increasing Northern Hemisphere insolation (Winograd et al., 1992; 1997). Termination II in particular remains contentious. U–Th dating results from the Bahamas also suggest that the mid-point age of the penultimate deglaciation is 135 ± 3 ka (Henderson and Slowey, 2000). Thus, the age of Termination II may have been forced by insolation in the Southern hemisphere, rather than in the Northern hemisphere as traditionally believed. Since the processes controlling Termination II were complexly interrelated, however, the age of the beginning of the last interglacial is suspect (Esat et al., 1999).

The orbitally tuned timescale is not a suitable test for the Milankovitch hypothesis because of the risk of circular reasoning. Those climate records with reliable chronology established by numerical dating or non-tuned age models can be used to test this hypothesis as independent controls. U-series dating of coral reefs in Henderson Island, tropical Pacific, suggests that the high-stand sea levels within MIS 9 are either

consistent with or slightly postdate the time of peak insolation at 333 ka at 65°N in July (Stirling et al., 2001). This supports the Milankovitch hypothesis. Generally, the major terminations at Shagou with an independent timescale are rapid, and closely correlated with July insolation maxima or increasing in Northern Hemisphere, as in the marine oxygen isotope records. The Shagou records show that during every termination, grain size changes are closely associated with Northern Hemisphere insolation, suggesting that insolation may be the primary forcing factor for the East Asian Monsoon by way of its impact on ice volume (Ding et al., 1995). Although the Milankovitch hypothesis contains many flaws and difficulties in explaining the influence of solar radiation on global climate, the records from the Shagou section and the ODP849 suggest that this influence, including terminations, does exist and is not an artificial phenomenon arising from orbital tuning.

Why, then, do the amplitudes of insolation and global climate not proportionally match? It seems unreasonable to assume that insolation is either the sole or the direct regulator for amplitude of climate changes, since insolation can be weak and the amplitudes are not matched. Increase of radiation in the Northern Hemisphere and other factors related to it might have caused the ice sheets to be unstable during the late stages of maximum ice volume. At Shagou, median grain size and the sand content fluctuated more frequently during cold periods than that during warm periods, especially in the upper part of the record corresponding to the late glacial with maximum ice volume. When the termination began, ice sheets in the Northern Hemisphere collapsed and melted, weakening the Siberian High. Then the winter monsoon declined and desert margins retreated, with the grain size of the loess sharply declining. However, the details of this mechanism are far from understood.

Lying very close to the Tengger and Badain Jaran Desert, and situated downwind of the drylands, the Shagou section also reflects desert evolution during the past 800 ka. Ding et al. (1999) has pointed out that a reduction in the size of dust source area and a decline in mean velocities of dust transporting winds led to a decline in particle size in eolian deposits, including loess. At Shagou, a decrease of grain size during deglaciation was caused by weak winter monsoon wind strengths and the retreat of the margin

of the Tengger and Badain Jaran deserts. The rapid terminations recorded in the Shagou section suggest that the winter monsoon, the westerlies, and the aridity of the ambient environment responded sensitively to solar insolation and ice volume.

6. Conclusion

When compared with other tuned and non-tuned results, the grain size age model is reliable for the past 800 ka for the Shagou loess section, although some uncertainties remain in this timescale. Grain size records from Shagou indicate that terminations are rapid, with the possible exception of Termination II. Termination VII shows the greatest amplitude. The timing of terminations at Shagou, using an independent timescale, is closely associated with either peak or increasing July solar insolation at 65°N, suggesting that insolation may be the trigger of terminations, though the mechanism remains unsolved. The unmatched amplitudes of change between the particle size record and insolation indicate that solar insolation may not be the sole regulator of the transition from glacial to interglacial climate of Chinese loess.

Acknowledgement

We are grateful to Edward Derbyshire for his valuable comments and correcting the text. We also thank Robert Jude for improving the English. This work is supported by National Natural Science Foundation of China (Grant No. 40301009), Innovation Foundation of Key Laboratory of Ice Core and Cold Regions Environment, and NNSFC (Grant No. 40171010).

References

- Bassinot, F.C., Labeyrie, L.D., Vincent, E., Quidelleur, X., Shackleton, N.J., Lancelot, Y., 1994. The astronomical theory of climate and the age of the Brunhes–Matuyama magnetic reversal. *Earth and Planetary Science Letters* 126, 91–108.
- Berger, A., Loutre, M.F., 1991. Insolation values for the climate of the last 10 million years. *Quaternary Science Reviews* 10, 297–317.
- Broecker, W.S., 1984. In: Berger, A., et al., (Eds.), *Terminations, in Milankovitch and Climate: Part 2*. D. Reidel, Norwell, MA, pp. 678–698.
- Burckle, L.H., 1993. Late Quaternary interglacial stages warmer than present. *Quaternary Science Reviews* 12, 825–831.
- Cande, S.C., Kent, D.V., 1995. Revised calibration of the geomagnetic polarity timescale for the Late Cretaceous and Cenozoic. *Journal of Geophysical Research* 100 (D), 603–6095.
- Derbyshire, E., Kemp, R.A., Meng, X.M., 1997. Climate change, loess and palaeosols: proxy measures and resolution in North China. *Journal of the Geological Society (London)* 154, 793–805.
- Ding, Z., Yu, Z., Rutter, N.W., Liu, T.S., 1994. Towards an orbital time scale for Chinese loess deposits. *Quaternary Science Reviews* 13, 39–70.
- Ding, Z.L., Liu, T.S., Rutter, N., Yu, Z.W., Guo, Z.T., Zhu, R.X., 1995. Ice-volume forcing of East Asian winter monsoon variations in the past 800,000 years. *Quaternary Research* 44, 149–159.
- Ding, Z.L., Sun, J.M., Rutter, N.W., Rokosh, D., Liu, T.S., 1999. Changes in sand of loess deposits along a North-South transect of the Chinese Loess Plateau and the implication for desert variation. *Quaternary Research* 52, 56–62.
- Esat, T.M., McCulloch, M.T., Chappell, J., Pillans, B., Omura, A., 1999. Rapid fluctuation in sea level recorded at Huon Peninsula during the penultimate deglaciation. *Science* 283, 197–201.
- Golsar, T., Arnold, M., Tisnerat-Laborde, N., Czernik, J., Wieckowski, K., 2000. Variations of Younger Dryas atmospheric radiocarbon explicable without ocean circulation changes. *Nature* 403, 877–880.
- Hays, J.D., Imbrie, J., Shackleton, N.J., 1976. Variations in the earth's orbit: pacemaker of the ice age. *Science* 194, 1121–1132.
- Henderson, G.M., Slowey, N., 2000. Evidence from U–Th dating against Northern Hemisphere forcing of the penultimate deglaciation. *Nature* 404, 61–66.
- Howard, W.R., 1997. A warm future of the past. *Nature* 388, 418–419.
- Kukla, G., An, Z.S., 1989. Loess stratigraphy in Central China. *Palaeogeography, Palaeoclimatology, Palaeoecology* 72, 203–225.
- Liu, T.S., et al., 1985. *Loess and Environment*. Since Press, Beijing (in Chinese).
- Liu, T.S., Ding, Z.L., Rutter, N., 1999. Comparison of Milankovitch periods between continental loess and deep sea records over the last 2.5 Ma. *Quaternary Science Reviews* 18, 1205–1212.
- Lotokaya, A., Ganssen, G.M., 1999. The structure of termination II (penultimate deglaciation and Eemian) in the North Atlantic. *Quaternary Science Reviews* 18, 1641–1654.
- Lu, H.Y., Guo, Z.T., Wu, N.Q., 1996. Paleomonsoon evolution and Heinrich events: evidence from the Loess Plateau and the South China Sea. *Quaternary Sciences* (1), 11–20 (in Chinese).
- Lu, H.Y., An, Z.S., Vandenberghe, J., Nugteren, G., Mingaarsn, N., Schwan, J., 1997. A dating model of loess stratigraphy in the central Chinese Loess Plateau and its preliminary application. *Acta Sedimentologica Sinica* 15 (3), 150–152 (in Chinese).

- Lu, H.Y., Liu, X.D., Zhang, F.Q., An, Z.S., Dodson, J., 1999. Astronomical calibration of loess–paleosol deposits at Luochuan, central Chinese Loess Plateau. *Palaeogeography, Palaeoclimatology, Palaeoecology* 154, 237–246.
- Martinson, D.G., Pisias, W.G., Hays, J.D., Imbrie, J., Moore, T.C., Shackleton, N.J., 1987. Age dating and the orbital theory of the ice age: development of a high resolution 0 to 300,000 year chronostratigraphy. *Quaternary Research* 27, 1–29.
- Muller, R.A., MacDonald, G.J., 1997. Glacial cycles and astronomical forcing. *Science* 277, 215–518.
- Pan, B.T., Wu, G.J., Wang, Y.X., Liu, Z.G., Guan, Q.Y., 2001. Age and genesis of Shagou River Terraces in Eastern Qilian Mountains. *Chinese Science Bulletin* 46 (6), 509–513.
- Petit, J.R., Jouzel, J., Raynaud, D., Barkov, N.I., Barnola, J.-M., Basile, I., Bender, M., Chappellaz, J., Davis, M., Delaygue, G., Delmotte, M., Kotlyakov, M., Legrand, M., Lipenkov, V.Y., Lorius, C., Pepin, L., Ritz, C., Saltzman, E., Stievenard, M., 1999. Climate and atmospheric history of the past 420,000 years from the Vostok ice core, Antarctica. *Nature* 399, 429–436.
- Porter, S.C., An, Z.S., 1995. Correlation between climate events in the North Atlantic and China during the last glaciation. *Nature* 375, 305–308.
- Raymo, M.E., 1997. The timing of major climate terminations. *Paleoceanography* 12 (4), 577–585.
- Raymo, M.E., Ruddiman, W.F., Shackleton, N.J., Oppo, D.W., 1990. Evolution of Atlantic–Pacific $\delta^{13}\text{C}$ gradients over the last 2.5 My. *Earth and Planetary Science Letters* 97, 353–368.
- Ruddiman, W.F., Raymo, M.E., Martinson, D.G., Clement, B.M., Backman, J., 1989. Pleistocene evolution: northern hemisphere ice sheet and North Atlantic Ocean. *Paleoceanography* 4 (4), 353–412.
- Seidenkrantz, M.-S., Bornmalm, L., Johnsen, S.J., Knudsen, K.L., Kuijpers, A., Lauritzen, S.-E., Leroy, S.A.G., Mergeai, I., Schweger, C., Vliet-Lanoc, B.V., 1996. Two-step deglaciation at the oxygen isotope stage 6/5e transition: the Zeifen–Kattegat climate oscillation. *Quaternary Science Reviews* 15, 63–75.
- Stirling, C.H., Esat, T.M., Lambeck, K., McCulloch, M.T., Blake, S.G., Lee, D.-C., Halliday, A.N., 2001. Orbital forcing of the marine isotope stage 9 interglacial. *Science* 291, 290–293.
- Vandenberghe, J., An, Z.S., Nugteren, G., Lu, H.Y., Van Huissteden, K., 1997. New absolute time scale for the Quaternary climate in the Chinese loess region by grain-size analysis. *Geology* 25 (1), 35–38.
- Winograd, I.J., Coplen, T.B., Landwehr, J.M., Riggs, A.C., Ludwig, K.R., Szabo, B.J., Kolesar, P.T., Revesz, K.M., 1992. Continuous 500,000-year climate record from vein calcite in Devils Hole, Nevada. *Science* 258, 255–260.
- Winograd, I.J., Landwehr, J.M., Ludwig, K.R., Coplen, T.B., Riggs, A.C., 1997. Duration and structure of the past four interglaciations. *Quaternary Research* 48, 141–154.
- Wu, N.Q., Rousseau, D.D., Liu, X.P., 2000. Response of mollusk assemblages from the Louchuan loess section to orbital forcing since the last 250 ka. *Chinese Science Bulletin* 45 (17), 1617–1622.
- Wu, G.J., Pan, B.T., Guan, Q.Y., Liu, Z.G., Li, J.J., 2002. Loess record of climatic changes during MIS5 in the Hexi Corridor, northwest China. *Quaternary International* 97–98, 167–172.